

Optical Frequency Mixing at Coupled Gold Nanoparticles

Matthias Danckwerts and Lukas Novotny*

Institute of Optics, University of Rochester, Rochester, New York USA

(Received 20 September 2006; published 10 January 2007)

We present nonlinear-optical four-wave mixing (4WM) at coupled gold nanoparticles. By decreasing the interparticle distance from large separation to touching contact, the 4WM yield increases by 4 orders of magnitude. The reason for this dramatic enhancement lies in the shift of the localized plasmon resonance to infrared wavelengths as the dimer is formed, making one of the input wavelengths doubly resonant. At the touching point, the 4WM signal changes discontinuously because of a sudden charge redistribution imposed by the formation of a conductive bridge. The 4-wave mixing signal provides an ultrasensitive measure for the contact point between a pair of particles and it can be employed as a spatially and temporally controllable photon source.

DOI: [10.1103/PhysRevLett.98.026104](https://doi.org/10.1103/PhysRevLett.98.026104)

PACS numbers: 68.37.Uv, 42.65.Ky, 73.20.Mf, 78.67.Bf

Noble-metal particles have received an ever increasing amount of scientific attention owing to their fascinating chemical and optical properties. Their optical response is governed by the resonant excitation of surface plasmons, and therefore depends on particle size, shape, and material, but also on the dielectric environment. Gold nanoparticles conjugated with specific biomolecules are used for DNA detection [1], biosensing, and imaging [2,3], and for drug delivery and cancer treatment [4,5]. Organic linker molecules can be employed for self-assembly of more complex nanostructures such as nanoparticle aggregates [6], metal-semiconductor hybrid structures [7], and for particle synthesis and immobilization [8]. Aggregates and ordered arrays of metal nanoparticles are being developed for controlled waveguiding of surface plasmons [9,10] and for surface enhanced spectroscopy [11,12].

To enhance the optical specificity of metal nanoparticles, a large body of research is devoted to tailoring their *linear* optical properties [13]. However, metal nanoparticles also exhibit a strong *nonlinear* response which is being applied, for example, in nanoparticle-doped dielectrics for frequency conversion [14,15]. The nonlinear susceptibility of the composite depends strongly on interactions between the particles as the percolation threshold is approached [16,17]. So far, most studies of the nonlinear properties of metal nanoparticles have been performed on particle ensembles or particle aggregates. However, ensemble averaged measurements often obscure important physical details because of size and shape variations as well as varying local environments and structural defects. Recent *single* nanoparticle studies have shown that ensemble averaging can be overcome and that the nonlinear-optical properties of individual and interacting nanoparticles can be measured [18,19].

In this Letter, we show that two near-infrared (NIR) laser frequencies (ω_1 and ω_2) can be very efficiently mixed at a pair of gold nanoparticles, yielding visible radiation at the frequency $2\omega_1 - \omega_2$, similar to surface-coherent anti-Stokes Raman scattering (CARS) [20]. By controllably

reducing the separation between the pair we demonstrate that the intensity of this four-wave mixing (4WM) signal can be enhanced by 4 orders of magnitude. Interestingly, at larger separations the 4WM signal increases continuously with decreasing separation but then, close to touching contact, abruptly changes to a different distance dependence. This discontinuity originates from the spectral jump of the surface plasmon resonance when the two particles get into conductive contact [21,22] and it provides an ultrasensitive optical measure for the contact point. The dimer acts as a strong emitter of light generated by optical wave mixing; its radiation is spectrally narrow and well separated from the excitation. With the dimer being attached to the end of a glass tip, we show that by scanning this probe over a sample surface, we can perform high-resolution near-field optical imaging and spectroscopy.

As shown in Fig. 1(a), we use an objective to focus two linearly polarized laser beams on the surface of a transparent sample with dispersed gold nanoparticles. The sample was prepared by spin coating a colloidal gold nanoparticle solution onto a glass coverslip which was first functionalized with (3-mercaptopropyl)trimethoxysilane (MPTMS). Another gold nanoparticle is attached to the end of an aminosilane functionalized pointed optical fiber [23,24] and its relative position with respect to the sample and the excitation beam is controlled in three dimensions with subnanometer accuracy using a shear-force feedback mechanism [25]. The light emitted from the nanoparticles is collected by the same objective and spectrally separated from the exciting light by a 45° dichroic beam splitter and other filters. For imaging and spectral analysis, either a single-photon counting avalanche photodiode (APD) or a combination of spectrometer and CCD detection is used. For excitation, a Ti:sapphire laser source produces ~180 fs pulses in the wavelength range of 700–900 nm at a repetition rate of 76 MHz. A part of this light is used to pump an optical parametric oscillator (OPO) to generate coherent pulses in the wavelength range of 1050–1200 nm. The two beams are combined and expanded to obtain approxi-

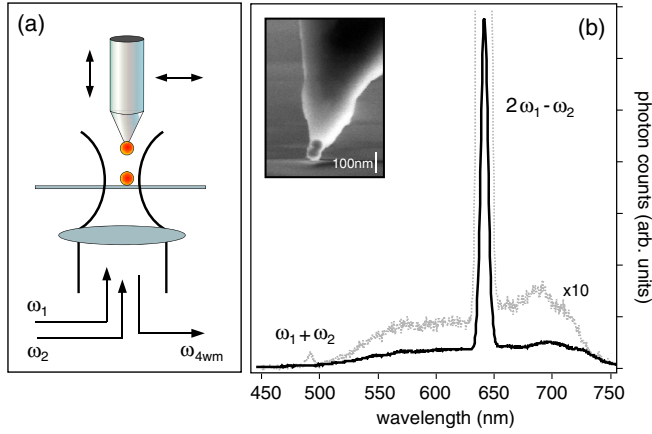


FIG. 1 (color online). (a) Sketch of the experiment. The nonlinear signal at frequency $2\omega_1 - \omega_2$ is measured as a function of the relative position between individual gold nanoparticles. (b) Emission spectrum from a dimer of two identical particles (60 nm diameter), excited with pulsed lasers of wavelength $\lambda_1 = 830$ nm and $\lambda_2 = 1185$ nm. The superimposed dotted curve shows the spectrum for two particles of unequal size (60 nm and 100 nm diameter). The inset shows an SEM image of two gold particles attached to a pointed optical fiber.

mately planar wave fronts at the back aperture of the objective. Average input beam powers at the back aperture are on the order of 0.5 mW corresponding to peak intensities of 1–10 GW/cm² at the sample.

The nonlinear-optical response of single isolated gold particles of 60 nm diameter is very weak for the intensities used in all our experiments. No significant harmonic generation nor wave mixing was observable; only a small background of continuum generation was measured [26]. This low yield is not surprising given the small source volume of the nanoparticles and the fact that the input wavelengths are not resonant with the surface plasmon resonance of the particles ($\lambda \approx 530$ nm). However, for a particle dimer we observe unusually strong four-wave mixing. A typical emission spectrum from a particle dimer attached to the end of a glass tip is shown in Fig. 1(b). Besides a weak continuum background the spectrum exhibits predominantly one emission line. The intensity of this line scales quadratically with the power of the Ti:sapphire laser and linearly with the power of the OPO and the spectral position is determined by $2\omega_1 - \omega_2$, ω_1 and ω_2 being the laser frequencies of Ti:sapphire and OPO, respectively. Consequently, this signal originates from a third-order polarizability

$$\mathbf{P}^{(3)}(2\omega_1 - \omega_2) = \vec{\chi}_3: \mathbf{E}_1(\omega_1)\mathbf{E}_1(\omega_1)\mathbf{E}_2(\omega_2), \quad (1)$$

similar to 4WM in nonlinear crystals. We have characterized many different particle dimers and found little variability in their 4WM yield and spectral response. Interestingly, because of the point symmetry of the geometry defined by two identical particles we see only very

weak χ_2 processes such as second-harmonic generation (SHG) or sum-frequency generation (SFG). The superimposed spectrum shown as a dotted curve in Fig. 1(b) originates from two particles of unequal diameters (60 nm and 100 nm). Because of the broken symmetry we now also observe SFG, but the intensity of the 4WM signal is still much stronger.

The 4WM conversion efficiency is highly polarization dependent. For a dimer, the signal is strongest when the excitation field is polarized along the dimer axis. This polarization dependence can be verified by raster scanning a vertical gold dimer over a bare glass surface and recording the 4WM intensity. The resulting 4WM image is characterized by two intense lobes (data not shown) oriented along the polarization direction of the two incident laser beams [18]. The two lobes represent the focal regions where the exciting fields are polarized along the dimer axis (longitudinal fields).

To understand the origin of the 4WM signal we have controllably varied the distance z between the two particles and monitored the signal yield. As shown in Fig. 1(a), a single sample particle was positioned into one of the two lobes of longitudinal field and a second particle, attached to a glass tip, was slowly approached from the top. The result of this measurement is shown in Fig. 2. For large particle-particle separations z we measure a count rate of roughly 80 s⁻¹, approximately 30–50 s⁻¹ out of which corresponds to the dark count level. As the separation is reduced the 4WM count rate first increases as $\sim z^{-1.8}$ and then abruptly transitions into a weaker z dependence around $z = 0.2$ nm (cf. inset). The transition point can be determined with an accuracy of ± 1 Å. This finding is consistent between measurements with different particle pairs.

At very close distances we observe fluctuations of the count rate because small changes in the contact region give rise to huge variations in the spectral response [22]. In most

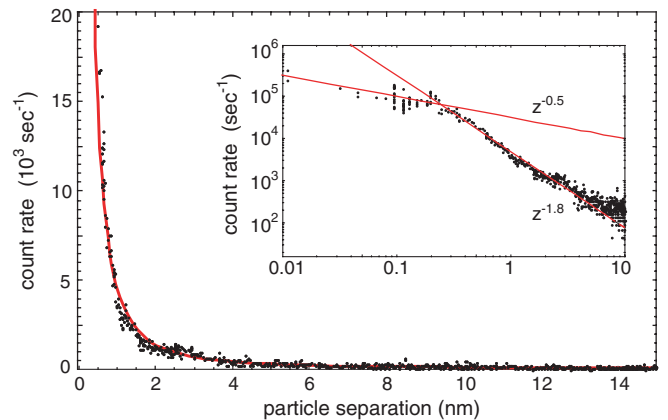


FIG. 2 (color online). (a) Four-wave mixing photon count rate ($\lambda = 639$ nm) as a function of the separation of two 60 nm gold nanoparticles. The inset shows a detailed view on a log-log scale. Dots are data and the curves are power-law fits.

cases, the particles cannot be separated once a dimer is formed, i.e., either the tip particle or the sample particle comes off and remains attached to the other particle as shown in the inset of Fig. 1(b). However, occasionally a release is possible and a trace can be recorded in the reverse direction. These reverse traces show a delayed response with a slight “snapping-off” behavior, similar to approach curves recorded with soft cantilevers in atomic force microscopy. This effect originates from the elasticity of the linker molecules used for particle immobilization.

The near-field coupling between two spheres has been calculated in the early 1980s by Aravind *et al.* [27] and Ruppin [28], but the contact point has been analyzed only recently [22,29]. Particle dimers have also been studied experimentally mainly by use of lithographic techniques [21,30–32]. To theoretically understand the plasmon resonances for particles near touching contact we have employed the multiple multipole (MMP) method [33] and calculated the local field distributions. The results shown in Fig. 3 indicate that the plasmon resonance is shifting towards longer wavelengths as the separation between the particles is decreased. Initially, this shift is rather weak: at $z = 1$ nm the resonance is found to be at $\lambda = 588$ nm, only redshifted by ~ 50 nm relative to the resonance of a single particle. On the other hand, as soon as the particles get near contact, the resonance abruptly shifts into the near infrared (cf. solid curve in Fig. 3). Consequently, the plasmon resonance becomes doubly resonant with the laser excitation at ω_1 ($\lambda = 830$ nm).

This abrupt leap of the resonance has been observed in extinction measurements [21] and recently analyzed by Romero *et al.* [22] who pointed out that the discontinuity

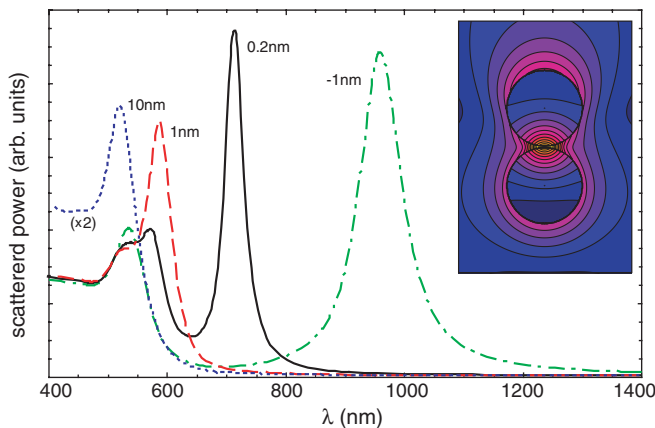


FIG. 3 (color online). Calculations of the elastically scattered power as a function of the separation z between two 60 nm gold particles excited with light polarized along the particle-particle axis ($z = 0$ corresponds to touching contact). The resonance shifts abruptly within $\Delta z \approx 0.5$ nm from the visible to the near-infrared thereby becoming doubly resonant with one of the excitation beams at touching contact. The inset shows the calculated field strength (E^2 , factor 2 between contour lines) for $z = 1$ nm.

at touching contact is due to a sudden charge redistribution required to ensure intraparticle charge neutrality. Consequently, as soon as a conductive bridge between the particles is formed, a previously unphysical mode suddenly becomes physical and the resonance undergoes a spectral jump.

The nonlinear polarization $\mathbf{P}^{(3)}$ increases strongly as the resonance shifts into the near infrared. Furthermore, because of the nonlinear nature of the 4WM signal the interaction range shrinks down to a subnanometer length scale as observed in our experiments. This makes the 4WM signal an ultrasensitive optical measure for the contact point. In agreement with Romero *et al.* we find that the fields near the contact region of two touching (penetrating) particles are remarkably strong and that the field strengths critically depend on slight geometrical variations. This finding is likely the reason for the observed fluctuations of the 4WM signal at touching contact. The curves in Fig. 3 also show higher-order resonances around $\lambda \approx 550$ nm. The wavelengths associated with these modes are not resonant with the exciting laser beams nor with the emitted 4WM signal and hence they have little influence on the signal yield. The shape of the higher-order resonances is slightly distorted because of interband transitions in the dielectric function of gold [34].

Interestingly, we find that the 4WM yield of a dimer can be even more enhanced by coupling to a third particle placed in close proximity to it. To demonstrate this effect we have attached two 60 nm particles to a glass tip (cf. Fig. 1(b) inset) and recorded the emitted 4WM intensity while raster scanning a sample with 60 nm gold particles underneath the dimer tip. The resulting optical 4WM intensity image is shown in Fig. 4(a). For the excitation powers used in our measurements the response from single nanoparticles is too weak to be detected and hence the optical contrast originates purely from the near-field coupling between a single particle and a particle dimer. The image in Fig. 4(a) shows that the contrast is enhanced at the edges of the sample particles. This phenomenon originates from the very strong distance dependence of the 4WM signal and the finite response of the shear-force feedback loop used to control the vertical position of the particle dimer tip.

An image of a cluster of three gold particles is shown in Fig. 4(b) and 4(c). While the topography clearly shows the lateral agglomeration of three nanoparticles, the 4WM image reveals that the signal is strongest when the dimer probe is placed between individual particles. In these configurations the dimer probe interacts simultaneously with two or three neighboring particles and the local fields become particularly strong. It is important to notice that the 4WM image represents the locally enhanced fields (hot spots) due to the particular interaction of sample (trimer) and probe (dimer) and that other images would result for other configurations.

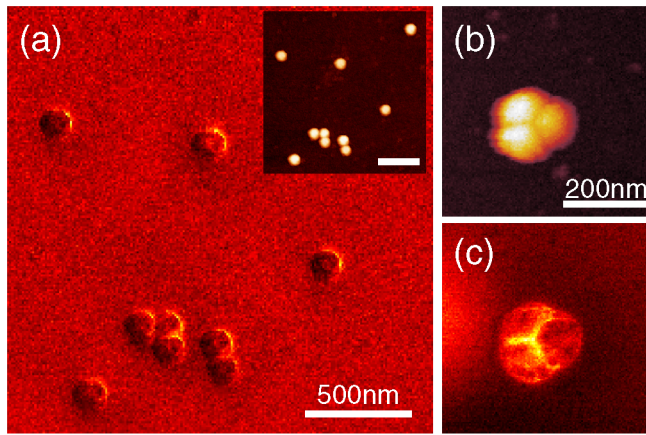


FIG. 4 (color online). (a) 4WM image recorded by raster-scanning a sample with individual gold particles underneath a stationary dimer tip. Inset shows the corresponding topographical image. (b), (c) A particle trimer imaged with a particle dimer tip. (b) Topography and (c) simultaneously recorded 4WM signal intensity.

In conclusion, we have demonstrated very efficient third-order nonlinear-optical frequency mixing at coupled gold nanoparticles. The 4WM yield increases by $\times 10^4$ as the interparticle distance is decreased to the contact point. At the contact point a conductive bridge is formed which gives rise to an abrupt jump of the plasmon resonance frequency into the near-infrared and which makes the 4WM distance dependence discontinuous. By controlling the interparticle distance we can generate bursts of narrow-band photons. Alternatively, a stable photon source is obtained by permanently joining two particles rigidly together. We have demonstrated that this source can be employed for high-resolution nonlinear near-field imaging. Further applications of these nonlinear photon sources are under investigation, including extinction spectroscopy and imaging.

We would like to thank Thomas Härtling and Michael R. Beversluis for initial experiments, and to Garnett W. Bryant and F. Javier García de Abajo for stimulating discussions. This work was supported by the US Department of Energy under Grant No. DE-FG02-01ER15204. M. D. acknowledges support from the Deutsche Akademie der Naturforscher Leopoldina, Grant No. BMBF-LPD 9901/8-103.

*Electronic address: <http://www.nano-optics.org>

[1] Y. C. Cao, R. Jin, and C. A. Mirkin, *Science* **297**, 1536 (2002).

- [2] D. J. Maxwell, J. R. Taylor, and S. M. Nie, *J. Am. Chem. Soc.* **124**, 9606 (2002).
- [3] C. Loo *et al.*, *Technol. Canc. Res. Treat.* **3**, 33 (2004).
- [4] J. H. Kim and T. R. Lee, *Drug Development Research* **67**, 61 (2006).
- [5] L. R. Hirsch *et al.*, *Ann. Biomed. Eng.* **34**, 15 (2006).
- [6] Y. Yang *et al.*, *Nanotechnology* **17**, 2821 (2006).
- [7] J. Lee *et al.*, *Nano Lett.* **4**, 2323 (2004).
- [8] R. W. J. Scott, O. M. Wilson, and R. M. Crooks, *J. Phys. Chem. B* **109**, 692 (2005).
- [9] A. Bouhelier *et al.*, *J. Phys. Chem. B* **109**, 3195 (2005).
- [10] B. Lamprecht *et al.*, *Phys. Rev. Lett.* **84**, 4721 (2000).
- [11] A. M. Michaels, J. Jiang, and L. E. Brus, *J. Phys. Chem. B* **104**, 11 965 (2000).
- [12] D. J. Anderson and M. Moskovits, *J. Phys. Chem. B* **110**, 13 722 (2006).
- [13] U. Kreibig and M. Vollmer, *Optical Properties of Metal Clusters* (Springer, New York, 1995).
- [14] R. J. Gehr and R. W. Boyd, *Chem. Mater.* **8**, 1807 (1996).
- [15] D. Y. Guan *et al.*, *J. Opt. Soc. Am. B* **22**, 1949 (2005).
- [16] R. del Coso *et al.*, *J. Appl. Phys.* **95**, 2755 (2004).
- [17] K. Li, M. I. Stockman, and D. J. Bergman, *Phys. Rev. B* **72**, 153401 (2005).
- [18] A. Bouhelier *et al.*, *Phys. Rev. Lett.* **90**, 013903 (2003).
- [19] M. Lippitz, M. A. van Dijk, and M. Orrit, *Nano Lett.* **5**, 799 (2005).
- [20] C. K. Chen *et al.*, *Phys. Rev. Lett.* **43**, 946 (1979).
- [21] T. Atay, J.-H. Song, and A. V. Nurmikko, *Nano Lett.* **4**, 1627 (2004).
- [22] I. Romero *et al.*, *Opt. Express* **14**, 9988 (2006).
- [23] T. Kalkbrenner *et al.*, *J. Microsc.* **202**, 72 (2001).
- [24] P. Anger, P. Bharadwaj, and L. Novotny, *Phys. Rev. Lett.* **96**, 113002 (2006).
- [25] K. Karrai and R. D. Grober, *Appl. Phys. Lett.* **66**, 1842 (1995).
- [26] M. R. Beversluis, A. Bouhelier, and L. Novotny, *Phys. Rev. B* **68**, 115433 (2003).
- [27] P. K. Aravind, A. Nitzan, and H. Metiu, *Surf. Sci.* **110**, 189 (1981).
- [28] R. Ruppin, *Phys. Rev. B* **26**, 3440 (1982).
- [29] S. Enoch, R. Quidant, and G. Badenes, *Opt. Express* **12**, 3422 (2004).
- [30] W. Rechberger *et al.*, *Opt. Commun.* **220**, 137 (2003).
- [31] L. Gunnarson *et al.*, *J. Phys. Chem. B* **109**, 1079 (2005).
- [32] D. ten Bloemendal *et al.*, *Plasmonics* **1**, 41 (2006).
- [33] L. Novotny and B. Hecht, *Principles of Nano-Optics* (Cambridge University Press, Cambridge, England, 2006).
- [34] P. B. Johnson and R. W. Christy, *Phys. Rev. B* **6**, 4370 (1972).